Thermal and electrical properties of Polyamide/Multi-Walled Carbon Nanotubes nanocomposites

E. Logakis[*], Ch. Pandis[*], V. Peoglos[*], P. Pissis[*], A. Kanapitsas[**], J. Pionteck[***], P. Pötschke[***], M. Mičušík[****] and M. Omastová[****]

[*] National Technical University of Athens, Zografou Campus, 15780, Athens, Greece, logmanos@central.ntua.gr
[**]Technological Educational Institute of Lamia, Department of Electronics, 35100 Lamia, Greece
[***]Leibniz Institute of Polymer Research Dresden, 01069 Dresden, Germany
[****]Polymer Institute, Slovak Academy of Sciences, 842 36 Bratislava, Slovakia

ABSTRACT

In this study composites of polyamide 6 and multiwalled carbon nanotubes (MWCNT) composites were prepared by diluting a masterbatch using melt mixing. Differential scanning calorimetry was employed in order to investigate the influence of nanotubes on the thermal transitions of polyamide 6. Significant changes are reported on crystallization and glass transition by the addition of nanotubes. The results are discussed in terms of polymer-filler interactions. Dielectric relaxation spectroscopy measurements were performed to study the electrical properties of the nanocomposites. Percolation threshold is calculated to be at 1.7 vol.% MWCNT.

Keywords: polyamide 6, carbon nanotubes, thermal transitions, electrical properties

1 INTRODUCTION

Among the nanoparticles carbon nanotubes (CNT), first described in 1991 by Iijima [1], have attracted considerable attention as new materials for mixing with polymers due to their very high aspect ratio (>1000), low density and exceptional electrical, mechanical and thermal properties. Polymer/CNT nanocomposites are promising materials with potential applications as electromagnetic shielding coatings, electrostatically dissipative materials, aerospace structural materials, and active elements in sensors [2].

Several processing methods are available for the production of polymer/CNT composites [2, 3]. Melt-mixing of CNT into thermoplastic polymers using conventional processing techniques are particularly desirable, because of the speed, simplicity, and availability in the plastic industry [2].

The purpose of this work is to examine the thermal, and electrical properties of multi-walled carbon nanotubes (MWCNT) filled polyamide 6 (PA6) nanocomposites formed by melt-mixing. To that aim differential scanning calorimetry and dielectric relaxation spectroscopy were employed. The influence of CNT on the thermal transitions of PA6 is investigated. The results are discussed in terms of nucleating action of CNT and interfacial polymer-filler interactions. Special attention is paid to percolation aspects [4] by *ac* conductivity measurements. Percolation threshold (p_c) is the critical concentration of the filler where conducting pathways are formed by CNT and consequently a transition from the insulating to the conducting phase is observed.

2 EXPERIMENTAL

2.1 Nanocomposites Preparation

A masterbatch of 20 wt.% MWCNT in PA6 was obtained from Hyperion Catalysis International in pellet form. The outside diameter of the tubes is approximately 10 nanometers and the length is over 10 microns giving a very high aspect ratio of ≥1000. Their density is approximately 1.75 g/cm^3 [5]. The masterbach was diluted with the same PA6 as used in the masterbach using melt mixing in a Plasti-Corder kneading machine (240°C, 15 min, 60 rpm). Prior to mixing, the materials were dried at 80°C in a vacuum for a minimum of 12h. Slabs with a thickness of 1 mm were formed by compression moulding of the mixed components using a laboratory hydraulic press (2.4 MPa, 240°C, 2 min). The final concentration of the samples in CNT varied from 2.5 to 20 wt.%. According to the material densities (1.15 g/cm^3 for PA6 and 1.75 g/cm^3 for CNT) the corresponding volume concentrations are 1.6 to 13.1 vol. %. It is noted that the same procedure was followed for both the pure PA and the masterbatch of 20 wt.% MWCNT in order to have comparable samples.

2.2 Differential Scanning Calorimetry

Differential scanning calorimetry (DSC) [6] measurements were carried out in the temperature range -50 to 250°C using a Perkin–Elmer Pyris 6 calorimeter. A heating and a cooling rate of 10 °C/min was used. It is noted that PA6 and its composite samples were formerly heated to 250°C and maintained there for 5 min to remove the previous thermal history and any water effects, as it is well known that PA6 is a hydrophilic polymer.

NSTI-Nanotech 2007, www.nsti.org, ISBN 1420061836 Vol. 2, 2007

2.3 Dielectric Relaxation Spectroscopy

Dielectric relaxation spectroscopy (DRS) [7] measurements were carried out isothermally in the frequency range 10^{-2}–10^{6} Hz and temperature range −150 to 100°C by means of a Novocontrol Alpha analyzer. The temperature was controlled with a Novocontrol Quatro cryosystem. Golden electrodes were sputtered on both sides of the samples, in order to assure good electrical contact.

3 RESULTS AND DISCUSSION

3.1 Thermal Transitions

Fig. 1 shows crystallization thermograms for the pure PA6 and its nanocomposites. For the neat PA6 only a single crystallization peak ($T_{c,1}$) is observed at about 185°C. For the PA6/MWCNT composites, the $T_{c,1}$ peak shifts to higher temperatures, 198°C, indicating that MWCNT act as nucleating agents. This behavior of CNT has been reported previously in literature in various polymeric matrices [8]. Additionally, a second crystallization peak ($T_{c,2}$) is observed at higher temperatures for the nanocomposites only, and its position gradually shifts to higher temperatures with a steady increase in magnitude at the same time as the concentration of MWCNTs increases. This indicates that the second $T_{c,2}$ peak is closely related to the addition of MWCNT to the PA6 matrix. The double crystallization peak in the nanocomposites can be interpreted by accepting either two different types of crystal structures or morphologies, or a two-step crystallization behavior. X-ray diffraction (XRD) and atomic force microscopy (AFM) measurements will be performed in future in order to clarify which of the above speculations applies.

In Fig. 2 melting thermograms (second heat) are presented for the neat PA6 and its nanocomposites. For the pure PA6 two main melting peaks are observed at 211 and 218°C. These peaks correspond to the melting of the γ and α crystallites of PA6, respectively [9]. It is well known that PA6 exhibits polymorphism behavior having three crystalline forms (α, β, and γ) which generally coexist [10]. A third peak is observed in Fig. 2 at about 205°C, possibly attributed to the melting of less perfect γ-crystallites. Contrary, for the nanocomposites only a single endotherm peak appears, indicating that the constraints from the CNT imposed on the polymeric chains favor the formation of the α-phase crystals [11]. The latter is very important as the α-crystallites constitute the more thermodynamically stable phase and exhibit better mechanical properties comparing with the γ-crystallites. Preliminary XRD measurements support the above ascertainment. Additionally, it is very interesting to note that the one-dimensional nanotubes seem to promote the α-phase crystals, whereas for two-dimensional fillers (such a clays) γ-phase crystals are more favorable [12]. This indicates the crucial role of the dimensionality of the inclusions, especially at nano-level, to the constraints imposed on the polymer chains and consequently to the final crystallization behavior. Furthermore, the melting peaks remain at the same position as the amount of MWCNT increases. Also, in the temperature region of 45-55°C a step in heat flow appears indicating the glass transition at the amorphous PA6 phase.

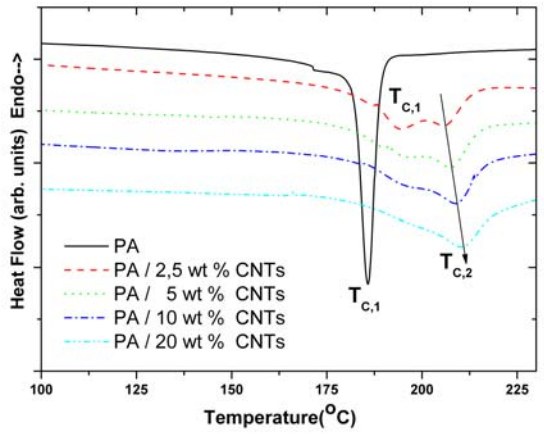

Fig. 1: Crystallization thermograms for the pure PA6 and for the nanocomposites indicated on the plot.

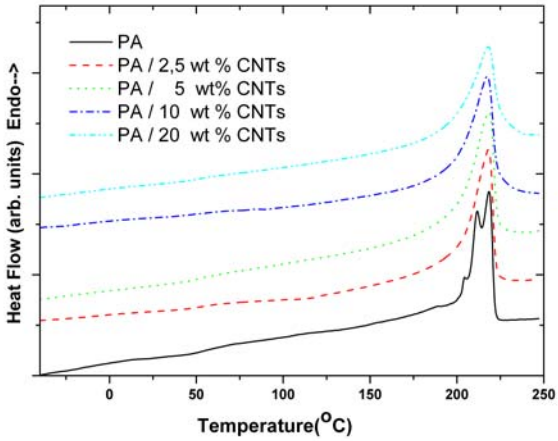

Fig. 2: Melting thermograms for the pure PA6 and for the nanocomposites indicated on the plot.

DSC results are summarized in Table 1, for the melting and crystallization and in Table 2 for the glass transition, where T_m is the melting temperature, $T_{c,1}$ and $T_{c,2}$ the crystallization temperatures, T_g the glass transition temperature, ΔH_m the heat of fusion, X_c the degree of crystallinity, ΔC_p the change of the heat capacity, and ΔT_g the width of glass transition. It should be noticed that ΔH_m, X_c and ΔC_p are normalized to the mass and to polymer content of each sample. ΔC_p^* is the ΔC_p normalized to the mass of the amorphous polymer by dividing with 1- X_c. The degree of crystallinity of PA6 is calculated from the following equation

$$X_c\,(\%) = \frac{\Delta H_m}{\Delta H_0} x100 \qquad (1)$$

where ΔH_o is the heat of fusion for 100 % crystalline PA6. ΔH_o for the α- and γ-form of PA6 are 241 and 239 J/g, respectively. An average value of 240 J/g was adopted in this study [10].

Sample	Melting			Crystallization	
	T_m (°C)	ΔH_m (J/g)	X_c (%)	$T_{c,1}$ (°C)	$T_{c,2}$ (°C)
PA	218.5	73.9	31	185.8	-
PA+2.5%CNT	217.9	88.4	37	194.4	205.6
PA+ 5%CNT	218.4	90.4	38	196.1	207.6
PA+ 10%CNT	217.6	99.8	42	197.0	208.9
PA+ 20%CNT	218.0	94.1	39	198.0	210.4

Table 1

The results in Table 1 show an increase of X_c with increasing the MWCNT amount in the composites. The relatively high cooling rate of 10 °C/min gives limited time to the polymer crystallization and as a result the addition of external nucleation sites, such as carbon nanotubes, leads to an increase of crystallization rate and consequently to an increase of the degree of crystallinity. This effect is more pronounced at low MWCNT contents. The sample with 20 wt.% deviates from this behavior indicating that for such high MWCNT contents the polymer cannot penetrate and crystallize to the agglomerates which are formed. Furthermore, the increase of the width of the melting peak shows the existence of a broader crystallite size distribution. MWCNT prevent the formation of large and perfect crystallites due to limited space and restrictions imposed to the motion of the PA6 chains.

Sample	Glass Transition			
	T_g (°C)	ΔC_p (J/g* °C)	ΔC_p^* (J/g* °C)	ΔT_g, (°C)
PA	56	0.17	0.25	8
PA+2.5%CNT	54	0.12	0.19	8
PA+ 5%CNT	52	0.13	0.21	8
PA+ 10%CNT	46	0.10	0.17	8
PA+ 20%CNT	49	0.07	0.11	10

Table 2

The results in Table 2 show a decrease in glass transition temperature and in heat capacity step as the amount of CNT increases, whereas the glass transition width remains practically unaffected. This behavior can be interpreted in terms of a two layer model [13]. According to this model an interfacial layer with partially or completely suppressed mobility is developed near to the CNT walls as a result of strong substance-constraint interactions [14]. Consequently, only one part of the polymer contributes to the glass transition and explains the reduction in ΔC_p which is presented in Table 2. This model also justifies the independence of the glass transition width, as the part of the polymer which participates in glass transition is not affected by the isolated MWCNT. Furthermore, the presence of MWCNT in the matrix, by preventing the packing of the polymer chains, induces an increase of the free volume and as a result increases the molecular mobility of the polymer chains allowing them to move even at lower temperatures. The latter justifies the observed reduction of the glass transition temperature in Table 2.

3.2 Electrical Properties

Fig. 3 shows the ac conductivity (σ_{ac}) at room temperature as a function of frequency for the samples indicated on the plot. The frequency dependence of the ac conductivity follows a power low behaviour and can be expressed by the following equation

$$\sigma'(\omega) = \sigma(0) + \sigma_{ac}(\omega) = \sigma_{dc} + A\omega^s \quad (2)$$

where ω is the angular frequency, σ_{dc} is the dc conductivity (at $\omega \rightarrow 0$), A is a constant which depends on temperature T, and s is an exponent dependent on both frequency and temperature with values in the range 0-1. This is a typical behavior for a wide variety of materials and is called 'universal dynamic response' (UDR) [15]. The value of σ_{dc} can be estimated from the plateau values of conductivity. Also, for each composition there is a critical frequency f_c beyond which a power law is followed. Due to space charge polarization a hump is appeared at the crossover region and the results cannot be further analyzed with the UDR theory.

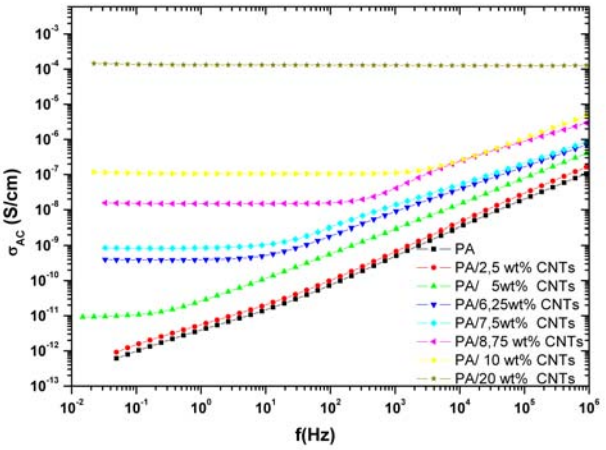

Fig. 3: Conductivity vs frequency for the samples indicated on the plot (concentrations correspond to wt%).

For the pure PA and PA/2.5 wt.% MWCNT, ac conductivity increases approximately linearly with the frequency in a logarithmic scale, exhibiting a typical capacitor behavior. At loadings in excess of 5 wt.% a dc plateau, where conductivity is independent of frequency, appears up to the critical frequency f_c. For these composites the value of the crossover frequency f_c increases with increasing MWCNT content. For the sample PA/20 wt.% MWCNT the dc plateau spreads to the whole frequency range. Thus, the dc conductivity plateau is clearly achieved above 2.5 and below 5.0 wt.% CNT indicating that

NSTI-Nanotech 2007, www.nsti.org, ISBN 1420061836 Vol. 2, 2007

percolation threshold (p_c), the transition from the insulating to the conducting phase, is located between 2.5-5.0 wt % (or 1.6-3.3 vol.%) MWCNT.

Fig. 4 shows the extrapolated values of the dc conductivity ($\sigma_{dc} = \sigma'(\omega \rightarrow 0)$) versus the MWCNT volume content (p) for the nanocomposites above the percolation threshold. In order to get an estimate for p_c the well known scaling law [4]:

$$\sigma_{dc}(p) \sim (p - p_c)^t \quad (3)$$

was fitted to the experimental σ_{dc} data for $p>p_c$, where t is a critical exponent which is related with the dimensionality of the investigated system. A value of $t \approx 2.0$ is predicted theoretically for a statistical percolation network in three dimensions [16]. The best linear fit for σ_{dc} vs. $(p- p_c)$ data on a log-log scale was found for $p_c = 1.7 \pm 0.1$ vol.% and critical exponent $t = 8.4 \pm 0.4$ (see inset in Fig. 4). The solid curve in Fig. 4 was calculated from Eq. (3) using the fit values of p_c and t.

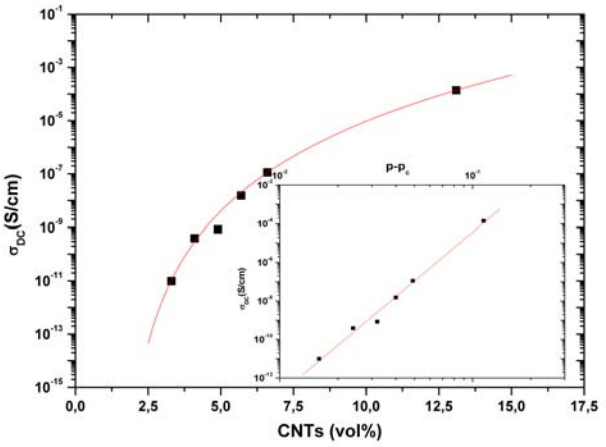

Fig. 4. σ_{dc} vs MWCNTs concentration p for nanocomposites above p_c. The inset shows a log-log plot of σ_{dc} vs $(p-p_c)$ with $t = 8.4$ and $p_c=1.7$ vol. %.

Such high values for t have been mentioned before in literature [17]. This discordance probably derives from the fact that, in contrast with the conventional percolation model, there is no physical contact between the fillers but the conducting CNT are connected electrically by tunneling and, as it has been proposed by Balberg [18], a very wide inter-particle distance distribution can lead to non-universal high t values. The absence of physical contacts between the nanotubes is supported from DSC results, where the formation of a polymer layer around the CNT walls prevents their formation. Also, the interaction between the nanotubes and the polymer matrix is not considered by the classic theory, constituting a second reason for the high value of the exponent in eq. 3.

4 CONCLUSIONS

The effect of MWCNTs on the thermal transition of PA6 was investigated. The results obtained indicate that MWCNTs act as nucleation agents and induce an increase in crystallization degree of PA6. Furthermore, their presence favors the formation of the more stable α-crystallites. As regards the glass transition, the observed reduction in T_g and ΔC_p is attributed to an increase of free volume and to an immobilized polymer part around the MWCNTs respectively.

By performing ac conductivity measurements and fitting the experimental data to the percolation threshold scaling low, the percolation threshold and critical exponent values were calculated ($p_c=1.7$ vol.% and $t=8.4$). The high exponent values indicate the absence of physical contacts between the nanotubes in agreement with DSC findings.

REFERENCES

[1] S. Iijima, Nature, 56, 354, 1991.
[2] O. Breuer and U. Sundararaj, Polymer Composites, 25, 630, 2004.
[3] N. Grossiord, J. Loos, O. Regev and C. E. Koning, Chemistry of Materials, 18, 1089, 2006.
[4] D. Stauffer and A. Aharony, "Introduction to percolation", Taylor and Francis, 1994.
[5] P. Pötschke, T. D. Fornes and D. R. Paul, Polymer, 43, 3247, 2002.
[6] T. Hatakeyama and F. X. Quinn, "Thermal Analysis", John Wiley & Sons Ltd, 1995.
[7] F. Kremer and A. Schoenhals, "Broadband dielectric spectroscopy", Springer, 2002.
[8] E. Assouline, A. Lustiger, A. H. Barber, C. A. Cooper, E. Klein, E. Wachtel and H. D. Wagner, Journal of Polymer Sciences Part B - Polymer Physics, 41, 520, 2003.
[9] T. Liu, I. Y. Phang, L. Shen, S. Y. Chow and W. D. Zhang, Macromolecules, 37, 7214, 2004.
[10] T. D. Fornes and D. R. Paul, Polymer, 44, 3945, 2003.
[11] I. Y. Phang, J. Ma, L. Shen, T. Liu and W. D. Zhang, Polymer International, 55, 71, 2006.
[12] D. M. Lincoln, R. A. Vaia, Z. G. Wang, B. S. Hsiao, Polymer, 42, 1621, 2001.
[13] G. Barut, P. Pissis, R. Pelster and G. Nimtz, Physical Review Letters, 80, 3543, 1998.
[14] J. A. Gomez Tejedor, C. J. Rodriguez Hernandez, J. L. Gomez Ribelles and M. Monleon Pradas, J Polym Sci B - Polym Phys, 46, 43, 2007.
[15] J. C. Dyre and T. B. Schroder, Reviews of Modern Physics, 72, 873, 2000.
[16] B. D. Gingold and C. J. Lobb, Physical Review B, 42, 8220, 1990.
[17] T. A. Ezquerra, M. Kulescza, C. Santa Cruz and F. J. Baltá Calleja, Advanced Materials., 2, 597, 1990.
[18] I. Balberg, Carbon, 40, 139, 2002.

Acknowledgement
The research was supported by ΠΕΝΕΔ 03ΕΔ150 and 03ΕΔ630 of ΓΓΕΤ and by the Slovak-German bilateral (rant number: D/05/15215).